J. Fluid Mech. (2009), *vol.* 638, *pp.* 5–26.
doi:10.1017/S0022112009991091

Particle dispersion by random waves in rotating shallow water

OLIVER BÜHLER AND MIRANDA HOLMES-CERFON†

Center for Atmosphere Ocean Science at the Courant Institute of Mathematical Sciences New York University, New York, NY 10012, USA

(Received 5 March 2009; revised 1 July 2009; accepted 2 July 2009)

We present a theoretical and numerical study of wave-induced particle dispersion due to random waves in the rotating shallow-water system, as part of an ongoing study of particle dispersion in the ocean. Specifically, the effective particle diffusivities in the sense of Taylor (*Proc. Lond. Math. Soc.*, vol. 20, 1921, p. 196) are computed for a small-amplitude wave field modelled as a stationary homogeneous isotropic Gaussian random field whose frequency spectrum is bounded away from zero. In this case, the leading-order diffusivity depends crucially on the nonlinear, second-order corrections to the linear velocity field, which can be computed using the methods of wave–mean interaction theory. A closed-form analytic expression for the effective diffusivity is derived and carefully tested against numerical Monte Carlo simulations. The main conclusions are that Coriolis forces in shallow water invariably decrease the effective particle diffusivity and that there is a peculiar choking effect for the second-order particle flow in the limit of strong rotation.

1. Introduction

The dispersion of particles due to random advection is a fundamental topic in fluid dynamics, with wide-ranging applications in geophysical and engineering flows. The fundamental theoretical analysis of such dispersion goes back to the groundbreaking studies on Lagrangian velocity statistics and scale-dependent pair dispersion by Taylor (1921) and Richardson (1926). Arguably, much of the work in this area has focused on turbulent flows, in which the random flow is specified at the outset. For example, a random velocity field may be defined via its space–time power spectrum together with additional modelling assumptions such as approximating the velocity field as a Gaussian random field. Based on these definitions, one can seek to compute quantities such as the one-particle effective diffusivity of Taylor (1921), who quantifies the variance growth of particle displacements (see § 2.1 for an exact definition). Even for a given velocity field, the resulting problem is far from trivial, not least because the velocity field is usually defined via its Eulerian, fixed-location properties, whereas for particle advection it is the Lagrangian, fixed-particle properties that are relevant. Still, a large body of theoretical, numerical and observational results is readily available in this area (e.g. Batchelor 1952; Kraichnan 1970; Chertkov *et al.* 1995; Majda & Kramer 1999; Sawford 2001; Toschi & Bodenschatz 2009).

A much less-studied case than the turbulent case arises if the random velocity field is due to small-amplitude waves described to leading order by linear theory. For

† Email address for correspondence: holmes@cims.nyu.edu

example, in oceanography, one might be interested in the horizontal dispersion of a passive tracer exposed to a spectrum of surface waves or in the analogous problem of quasi-horizontal dispersion along stratification surfaces due to a spectrum of internal gravity waves at depth. It is then easy to show that if there is no wave energy at zero wave frequency, then the diffusivity of particles due to the linear wave motion alone is zero. This situation is, in fact, generic for inertia–gravity waves, whose frequencies are bounded away from zero by the Coriolis parameter.

The leading-order dispersion then occurs at a higher order in wave amplitude, i.e. it is then essential to take nonlinear corrections to the linear velocity field into account in order to obtain a self-consistent Lagrangian velocity field for the particles. In other words, beginning with a statistical description of the linear wave field, the task of finding the statistical description of the Lagrangian velocity field is itself a non-trivial part of the solution. Basically, one needs to compute both the Stokes drift and the second-order Eulerian flow correction in order to arrive at the second-order Lagrangian flow that moves the particles. This makes computing the particle dispersion due to small-amplitude waves a problem in wave–mean interaction theory. For example, the relevant equations can be viewed as extensions of the mean-flow equations governing the non-dissipative wave–mean interactions studied by Bühler & McIntyre (1998), which were, however, derived under the restriction to slowly varying wavetrains. This restriction is generally not appropriate for random waves.

Since only the second-order velocity corrections contribute, the diffusion that results is fourth-order in wave amplitude. Hence, if vortical modes are present at the same order as the waves, one would expect them to induce a ballistic motion, which could dominate the wave diffusion. Other types of particle transport can also compete with wave diffusion if certain assumptions on the wave field are satisfied. In wave fields that are compressible and anisotropic, particles may experience a second-order drift velocity, which can significantly alter the particle transport (Balk 2006). Another interesting effect is particle segregation, whereby under suitable conditions compressible wave fields can give rise to small-scale density inhomogeneities (Balk, Falkovich & Stepanov 2004; Vucelja, Falkovich & Fouxon 2007). We would like to highlight the properties of the fourth-order wave-induced diffusivity, so we focus on isotropic velocity fields with no vorticity, in particular those induced by a small-amplitude linear wave field.

Our own interest in this problems stems from oceanographic observation of horizontal diffusivities on the sub-mesoscale, i.e. on horizontal scales of 1–10 km. Specifically, during the North Atlantic Tracer Release Experiment (Ledwell, Watson & Law 1993; Ledwell, Watson & Law 1998), a passive tracer was released at 300 m depth in the ocean and measured over several months to spread horizontally with an effective diffusivity of about 2 $m^2\ s^{-1}$ on horizontal scales of 1–10 km. Since molecular diffusivity is on the order of $10^{-9}m^2\ s^{-1}$, larger-scale physical processes must be responsible for this horizontal spreading, but it is fair to say that so far no conclusive answer as to which process is involved has emerged. For instance, some of the diffusivity could come from the interaction of internal waves with small vortical modes (Polzin & Ferrari 2004). Another hypothesis, not yet adequately tested, is that internal waves interacting with themselves can induce a horizontal diffusivity of this magnitude.

We are aware of only a handful of previous studies of wave-induced diffusivity. In Herterich & Hasselmann (1982), effective diffusivities were computed for surface waves by using a framework based on off-resonant wave–wave interactions. This is a challenging problem because the usual surface wave spectra, such as the JONSWAP

spectrum, are highly anisotropic, which leads to particle dispersion that includes a net drift as well as diffusion. Sanderson & Okubo (1988) used a similar approach for horizontally isotropic internal gravity waves in the non-rotating Boussinesq equations. However, the absence of Coriolis forces severely limits the utility of their calculation to ocean data, which invariably shows most wave activity near the inertial frequency. Finally, Weichman & Glazman (2000) developed a general formalism for computing the diffusivity in weakly nonlinear systems, which does include rotating systems. However, it appears that their formalism is based entirely on the dispersion relation and does not use the nonlinear parts of the fluid equations. This suggests that their findings are restricted to Stokes drift effects, so they do not include the complete Lagrangian flow. Presumably, this explains their own peculiar finding, namely that their results predict a non-zero diffusivity even in a one-dimensional situation, where it is clear on kinematic grounds that particles cannot separate in the long run without reducing the overall fluid density. It is precisely such mass-conservation effects that are missing if one considers only the Stokes drift. Common to all of these studies is the overall complexity of the required manipulations in both Fourier and real space and the need to estimate high-dimensional integrals numerically in order to compute the diffusivities.

Now, we study the horizontal diffusion induced by a random wave field in the rotating shallow-water equations as an idealized testbed and stepping stone for an ongoing extension of this work to the rotating three-dimensional Boussinesq equations. In our model, the wave field is a stationary isotropic homogeneous Gaussian random field defined by its power spectrum. We view this as a crude model for a real wave spectrum that is in forced–dissipative equilibrium. Even this simple model for a linear velocity field leads to a second-order Eulerian flow and Stokes correction that are non-Gaussian, so non-trivial methods are required to evaluate the Lagrangian velocity.

Our study differs from previous ones in three ways: (i) we find a real-space equation for the Lagrangian velocity field as a sum of an Eulerian flow and a Stokes correction; (ii) we obtain an analytic expression for the diffusivity as a function of the scale of the wavenumber spectrum of the waves; and (iii) we verify our calculations with numerical Monte Carlo simulations. Indeed, in our experience this independent numerical test on the results was essential for establishing the correct form of the somewhat daunting algebraic manipulations involved in calculating the diffusivity.

The analytic expression for the diffusivity is scale-selective, i.e. it depends on the Rossby deformation scale associated with the Coriolis force. Our principal result here is that the Coriolis force invariably reduces the effective particle diffusivity induced by the waves. In particular, for strong rotation the diffusivity drops off very sharply. Further investigation shows that this is because of a choking effect in which the second-order Lagrangian flow is sharply reduced in magnitude compared with the Stokes drift and the Eulerian flow, which separately are much larger, but nearly cancel each other. Clearly, this choking effect would be entirely missed if only the Stokes drift were considered.

The structure of the paper is as follows. In § 2, we outline the kinematics of particle dispersion and the governing equations that will be used in the paper, in § 3 we describe in detail the mathematical formalism that will be used to represent the random wave field, and in § 4 we compute the Lagrangian velocity field and the associated effective diffusivity. In § 5, we analyse the dependence of the diffusivity on rotation and in § 6 we describe the Monte Carlo simulations for the one-particle and two-particle diffusivities. Finally, some concluding comments are offered in § 7.

2. Particle dispersion and fluid equations

We consider the simplest measure of particle dispersion, namely the particle diffusivity associated with the displacement variance as introduced by Taylor (1921). The plan is to evaluate this diffusivity in the context of small-amplitude waves in the rotating shallow-water equations. To prepare the ground for this, we summarize the relevant definitions and governing equations in this section.

2.1. *Kinematics of particle dispersion*

We consider a collection of particles with Cartesian positions $X_i(t)$ and random Lagrangian velocities $u_i(t) = \mathrm{d}X_i(t)/\mathrm{d}t$. For a stationary homogeneous zero-mean velocity field, each particle's expected position is its initial position. Then

$$\frac{1}{2}\frac{\mathrm{d}}{\mathrm{d}t}\mathbb{E}(X_i(t) - X_i(0))(X_j(t) - X_j(0)) = \int_0^t \tilde{R}_{ij}(\tau)\,\mathrm{d}\tau, \tag{2.1}$$

where $\mathbb{E}$ denotes expectation and

$$\tilde{R}_{ij}(\tau) = \frac{1}{2}(\mathbb{E}\overline{u_i(t)}u_j(t+\tau) + \mathbb{E}\overline{u_j(t)}u_i(t+\tau)).$$

Here, the overbar is complex conjugation; we use this notation because it simplifies certain calculations later. Assuming isotropic velocity statistics and convergence as $t \to \infty$, the right-hand side of (2.1) becomes $D_u\delta_{ij}$, where

$$D_u \equiv \int_0^\infty C_{u,u}(\tau)\,\mathrm{d}\tau, \quad \text{and} \quad C_{u,u}(\tau) \equiv \mathbb{E}\overline{u(t)}u(t+\tau). \tag{2.2}$$

Here, u is an arbitrary Cartesian component of the velocity vector. By definition, D_u is the single-particle diffusivity induced by the random flow; it measures the absolute particle dispersion. Two other ways of expressing the diffusivity are useful. First, observing that $D_u = \int_{-\infty}^{\infty} C_{u,u}(\tau)\,\mathrm{d}\tau/2$, we see that the diffusivity is proportional to the Fourier transform of the covariance function evaluated at zero frequency. Specifically, using the convention

$$\hat{C}_{u,u}(\omega) = \int_{-\infty}^{\infty} \mathrm{e}^{-\mathrm{i}\omega\tau} C_{u,u}(\tau)\,\mathrm{d}\tau \quad \text{and} \quad C_{u,u}(\tau) = \frac{1}{2\pi}\int_{-\infty}^{\infty} \mathrm{e}^{\mathrm{i}\omega\tau}\hat{C}_{u,u}(\omega)\,\mathrm{d}\omega \tag{2.3}$$

we have

$$D_u = \frac{1}{2}\hat{C}_{u,u}(0). \tag{2.4}$$

Second, if we define the velocity auto-correlation time to be

$$\tau_u = \frac{1}{2}\int_{-\infty}^{\infty} \frac{C_{u,u}(\tau)}{C_{u,u}(0)}\,\mathrm{d}\tau \quad \text{then} \quad D_u = \mathbb{E}|u|^2\tau_u. \tag{2.5}$$

Relative particle dispersion is measured by multi-particle diffusivities, which are defined in analogy with (2.1) and (2.2) (e.g. Batchelor 1952). For example, the two-particle diffusivity tensor $D^{(2)}_{ij}$ is based on the distance $\Delta_i(t) = X_i(t) - Y_i(t)$ between two distinct particle trajectories $X_i(t)$ and $Y_i(t)$ such that

$$\lim_{t\to\infty}\frac{1}{2}\frac{\mathrm{d}}{\mathrm{d}t}\mathbb{E}(\Delta_i(t) - r_i)(\Delta_j(t) - r_j) = D^{(2)}_{ij}(r_k) \quad \text{with} \quad r_i = \Delta_i(0). \tag{2.6}$$

Returning to the one-particle diffusivity, we note a very useful fact: if the velocity field contains a component that is the time derivative of some stationary random field, then this component does not contribute to the diffusivity. To demonstrate this,

we let $u = U + V_t$, where U, V are stationary random variables, V is differentiable, and their correlation and cross-correlation functions decay at ∞. It follows that

$$2D_u = \int_{-\infty}^{\infty} \mathbb{E}\overline{u(t)}u(t+\tau)\,\mathrm{d}\tau = \int_{-\infty}^{\infty} (C_{U,U}(\tau) + C_{V_t,V_t}(\tau) + C_{U,V_t}(\tau) + C_{V_t,U}(\tau))\,\mathrm{d}\tau.$$

Using $C_{V_t,V_t}(\tau) = -\mathrm{d}^2/\mathrm{d}\tau^2\, C_{V,V}(\tau)$, $C_{U,V_t}(\tau) = \mathrm{d}/\mathrm{d}\tau\, C_{U,V}(\tau)$, $C_{V_t,U}(\tau) = -\mathrm{d}/\mathrm{d}\tau\, C_{V,U}(\tau)$ (see Yaglom 1962) and the decay at ∞ gives

$$2D_u = 2D_U - \frac{\mathrm{d}}{\mathrm{d}t} C_{V,V}|_{-\infty}^{\infty} + C_{U,V}|_{-\infty}^{\infty} - C_{V,U}|_{-\infty}^{\infty} = 2D_U. \tag{2.7}$$

Thus, $D_u = D_U$ as claimed. This will allow numerous simplifications in the computations.

2.2. *Governing fluid equations and asymptotic expansion*

We work with a slight generalization of the standard rotating two-dimensional shallow-water equations on an infinite flat domain:

$$\boldsymbol{u}_t + \boldsymbol{u}\cdot\nabla\boldsymbol{u} + f\hat{\boldsymbol{z}}\times\boldsymbol{u} + g\nabla(\mathscr{L}h) = 0, \tag{2.8}$$

$$h_t + \nabla\cdot(h\boldsymbol{u}) = 0. \tag{2.9}$$

Here, $\boldsymbol{x} = (x, y)$ are the horizontal coordinates, t is time, f is the Coriolis parameter, $\hat{\boldsymbol{z}}$ is the vertical unit vector, g is gravity, $\boldsymbol{u} = (u, v)$ is the velocity field and h is the layer depth. The generalization is that we allow a linear operator $\mathscr{L}$ to act on the height field in the pressure term. The operators $\mathscr{L}$ that we consider are defined by their real Fourier symbols $\hat{L}$ such that

$$\mathscr{L}\exp(\mathrm{i}[kx + ly]) = \hat{L}(\boldsymbol{k})\exp(\mathrm{i}[kx + ly]) \tag{2.10}$$

for a Fourier mode with wavenumbers $\boldsymbol{k} = (k, l)$. The standard shallow-water equations are included by setting $\hat{L} = 1$, whilst other choices of $\hat{L}$ change the linear dispersion relation, thus providing us with a crude way of incorporating the dispersive effects of additional physics such as surface tension or finite layer depth (e.g. Whitham 1974). Throughout, we will restrict ourselves to isotropic operators $\mathscr{L}$ such that $\hat{L}(\boldsymbol{k})$ is a function of $\kappa = |\boldsymbol{k}|$ only.

An important property of the inviscid equations is the material conservation of potential vorticity (PV), i.e.

$$q_t + \boldsymbol{u}\cdot\nabla q = 0, \quad \text{where} \quad q = \frac{\nabla\times\boldsymbol{u} + f}{h} = \frac{v_x - u_y + f}{h}. \tag{2.11}$$

In particular, if at the initial time q takes a uniform value f/H, say, then it will remain at this value at all later times. This leads to the exact nonlinear PV constraint

$$q = \frac{f}{H} \quad \Leftrightarrow \quad \nabla\times\boldsymbol{u} = \frac{h - H}{H} f. \tag{2.12}$$

For rotating flow, this quantifies the familiar 'ballerina' effect due to stretching of background vorticity.

We seek solutions to (2.8) and (2.9) as an asymptotic expansion in powers of a small-amplitude parameter $a \ll 1$. We assume no motion at leading order, so the $O(1)$ velocity field is zero and the $O(1)$ height field is a constant $h = H$. At $O(a)$, the flow is a random wave field satisfying the linearized versions of (2.8) and (2.9). The nonlinear interactions between the waves generate flow corrections at higher orders, which we will calculate at $O(a^2)$. Therefore, using a subscript n to represent

contributions at $O(a^n)$, our solution takes the form

$$\begin{pmatrix} \boldsymbol{u} \\ h \end{pmatrix} = \begin{pmatrix} \boldsymbol{0} \\ H \end{pmatrix} + a \begin{pmatrix} \boldsymbol{u}_1 \\ h_1 \end{pmatrix} + a^2 \begin{pmatrix} \boldsymbol{u}_2 \\ h_2 \end{pmatrix} + O(a^3). \tag{2.13}$$

This asymptotic flow set-up is reminiscent of small-amplitude wave–mean interaction theory, but in our case, flow averaging is not necessary and hence we will do without the unnecessary complication of introducing a mean–disturbance decomposition in (2.13). Under the assumption that there is a non-zero frequency cut-off (which is automatically satisfied if $f \neq 0$), the linear $O(a)$ wave field does not contribute to the particle diffusivity. To see this, let $\xi = \int u_1 \,\mathrm{d}t$ be the $O(a)$ displacement field and note that the frequency cut-off means that ξ is a stationary random variable with bounded variance. Therefore, $u_1 = \partial_t \xi$, so $D_{au_1+a^2u_2} = D_{a^2u_2}$ by (2.7). We therefore expect a leading-order diffusivity at $O(a^4)$, which is due to the $O(a^2)$ Lagrangian velocity field. Before moving on, we note that a regular perturbation expansion such as (2.13) can be expected to be valid for an $O(1)$ time scale as $a \to 0$. Basically, we assume that $a \ll 1$ is small enough such that the expansion is valid for the duration of the $O(1)$ auto-correlation time scale of the second-order Lagrangian velocity field to be computed.

3. Random linear wave field

The natural representation of a stationary Gaussian field in spectral space involves a few technicalities, which we spell out in a scalar example in the next section, before describing the full wave field in § 3.2.

3.1. *Scalar example of spectral representation*

We first consider a scalar random field $u(x)$ as a function of a single variable $x \in \mathbb{R}$ and then extend this to a time-dependent field $u(x,t)$ constrained by a dispersion relation. Now, there is a technical problem concerning Fourier transforms of stationary random functions because if one uses the standard transform (2.3) as in

$$\hat{u}(k) = \int_{-\infty}^{\infty} \mathrm{e}^{-\mathrm{i}kx} u(x) \,\mathrm{d}x \quad \text{and} \quad u(x) = \frac{1}{2\pi} \int_{-\infty}^{\infty} \mathrm{e}^{\mathrm{i}kx} \hat{u}(k) \,\mathrm{d}k, \tag{3.1}$$

then $\hat{u}(k)$ almost surely does not exist. One way to see this is via Parseval's theorem, which states that the integral of $|\hat{u}|^2$ over k equals the integral of $2\pi|u|^2$ over x. The latter is infinite for any homogeneous random function $u(x)$ regardless of its spectral bandwidth, which implies that $\hat{u}$ is infinite for all k. One can deal with this problem either by restricting to a bounded periodic domain at the outset or by using a measure-valued notion of a Fourier transform (e.g. Yaglom 1962; Yaglom 1987). We adopt the second approach, as it allows us to retain the generality of the problem without introducing another length scale, yet it is easy to adapt to a bounded periodic domain for numerical simulations as in § 6. Thus, we replace (3.1*b*) by

$$u(x) = \frac{1}{2\pi} \int_{-\infty}^{\infty} \mathrm{e}^{\mathrm{i}kx} \,\mathrm{d}\hat{u}(k), \tag{3.2}$$

where for a stationary field $u(x)$, the random spectral measure $\mathrm{d}\hat{u}(k)$ is defined by

$$\mathbb{E}\,\mathrm{d}\hat{u}(k) = 0, \;\; \frac{1}{2}\mathbb{E}\,\overline{\mathrm{d}\hat{u}(k)}\,\mathrm{d}\hat{u}(k') = 2\pi E(k)\delta(k-k')\,\mathrm{d}k\,\mathrm{d}k', \;\; \frac{1}{2}\mathbb{E}\,|\mathrm{d}\hat{u}(k)|^2 = 2\pi E(k)\,\mathrm{d}k. \tag{3.3}$$

For real $u(x)$, we also have $\mathrm{d}\hat{u}(-k) = \overline{\mathrm{d}\hat{u}(k)}$. The factor $1/2$ maintains consistency with the conventional definition of energy density as $u^2/2$. The real function $E(k) \geqslant 0$ is the power spectrum of $u(x)$, which, by (3.2)–(3.3), is also half of the Fourier transform of the covariance function:

$$\frac{1}{2}C_{u,u}(s) = \frac{1}{2}\mathbb{E}\,\overline{u(x)}u(x+s) = \frac{1}{2\pi}\int_{-\infty}^{\infty} \mathrm{e}^{\mathrm{i}ks}\,E(k)\,\mathrm{d}k. \tag{3.4}$$

Thus, $\hat{C}_{u,u}(k) = 2E(k)$ in the notation of (2.3). The relations (3.2)–(3.4) hold for any stationary random function $u(x)$, but in the particular case of a Gaussian function, the probability distribution for the real and imaginary parts of $\mathrm{d}\hat{u}(k)$ is independent identical normal distribution with mean zero and variance according to (3.3).

The natural extension of (3.2) to a time-dependent field $u(x,t)$ is

$$u(x,t) = \frac{1}{(2\pi)^2}\int \mathrm{e}^{\mathrm{i}(kx+\omega t)}\,\mathrm{d}\hat{u}(k,\omega) \tag{3.5}$$

with $\mathbb{E}\,\mathrm{d}\hat{u}(k,\omega) = 0$,

$$\frac{1}{2}\mathbb{E}\,\overline{\mathrm{d}\hat{u}(k,\omega)}\,\mathrm{d}\hat{u}(k',\omega') = (2\pi)^2 E(k,\omega)\delta(k-k',\omega-\omega')\,\mathrm{d}k\,\mathrm{d}k'\,\mathrm{d}\omega\,\mathrm{d}\omega', \tag{3.6}$$

and $\hat{C}_{u,u}(k,\omega) = 2E(k,\omega)$ for the Fourier transform of $C_{u,u}(s,\tau) = \mathbb{E}\overline{u(x,t)}u(x+s,t+\tau)$. The marginal one-dimensional spectrum $E(k)$ is as follows:

$$E(k) = \frac{1}{2\pi}\int E(k,\omega)\,\mathrm{d}\omega. \tag{3.7}$$

Here, the factor 2π ensures consistency in

$$\frac{1}{2}C_{u,u}(0,0) = \frac{1}{2}\mathbb{E}|u|^2 = \frac{1}{(2\pi)^2}\int E(k,\omega)\,\mathrm{d}k\,\mathrm{d}\omega = \frac{1}{2\pi}\int E(k)\,\mathrm{d}k. \tag{3.8}$$

Now, constraining every realization of $u(x,t)$ to solve a linear wave problem means constraining the admissible frequency values by a dispersion relation of the form $\omega = \omega_0(k)$, say. This leads to

$$\mathrm{d}\hat{u}(k,\omega) = 2\pi\delta(\omega-\omega_0(k))\,\mathrm{d}\hat{u}(k)\,\mathrm{d}\omega \quad \text{and} \quad E(k,\omega) = 2\pi\delta(\omega-\omega_0(k))E(k), \tag{3.9}$$

which can be checked for consistency with both (3.6) and (3.7). More generally, if there are N frequency branches, then there are N terms in (3.9) and these could have different energy spectra $E_n(k)$ with $n \leqslant N$. In particular, if there are $N = 2$ equal-and-opposite branches $\omega = \pm\omega_0(\kappa)$ with $\kappa = |\boldsymbol{k}|$ that are statistically independent and identically distributed, then a compact representation for $u(x,t)$ follows by assuming that $\mathrm{d}\hat{u}(k,\omega)$ satisfies (3.6) with

$$E(k,\omega) = 2\pi\left[\delta(\omega-\omega_0(\kappa)) + \delta(\omega+\omega_0(\kappa))\right]\frac{1}{2}E(k). \tag{3.10}$$

The factor $1/2$ means $E_1(k) = E_2(k) = E(k)/2$. Multi-component and multi-dimensional random wave fields can now be defined in analogy with $u(x,t)$ whilst adjusting powers of 2π and so on as needed.

3.2. *Wave field representation*

Based on the foregoing, the $O(a)$ wave fields are written as

$$\begin{pmatrix} u_1 \\ v_1 \\ h_1 \end{pmatrix} = \frac{1}{(2\pi)^3} \int \mathrm{e}^{\mathrm{i}(kx+ly+\omega t)} \begin{pmatrix} \mathrm{d}\hat{u} \\ \mathrm{d}\hat{v} \\ \mathrm{d}\hat{h} \end{pmatrix}, \tag{3.11}$$

where $\mathrm{d}\hat{u}$, $\mathrm{d}\hat{v}$, $\mathrm{d}\hat{h}$ are random measures on the dual space $\{(k,l,\omega) \in \mathbb{R}^{3*}\}$. Gaussianity of the wave field implies that these measures are also Gaussian. They are not necessarily independent, but the vector of measures can be decomposed into a basis of three orthogonal, independent modes, which can be calculated from the linearized shallow-water equations. Each of these is singularly supported on a subset $\{\omega = \omega(k,l)\} \subset \mathbb{R}^{3*}$ corresponding to a particular branch of the dispersion relation. One of these branches corresponds to the balanced vortical mode with $\omega = 0$, which is associated with a non-zero potential vorticity disturbance and which we do not consider any further. The other two branches satisfy $\omega = \pm\omega_0(\kappa)$, where

$$\omega_0(\kappa) = +\sqrt{\kappa^2 c^2 \hat{L}(\kappa) + f^2} \tag{3.12}$$

is the dispersion relation for inertia–gravity waves in shallow water. Here, $c^2 = gH$ and (κ,θ) are polar coordinates for $\boldsymbol{k} = (k,l) = \kappa(\cos\theta, \sin\theta)$. Both branches are represented using a Gaussian random measure $\mathrm{d}\hat{\phi}(\boldsymbol{k},\omega)$ such that

$$\mathbb{E}\mathrm{d}\hat{\phi}(\boldsymbol{k},\omega) = 0, \qquad \begin{pmatrix} \mathrm{d}\hat{u} \\ \mathrm{d}\hat{v} \\ \mathrm{d}\hat{h} \end{pmatrix} = \begin{pmatrix} -\cos\theta + \mathrm{i}\frac{f}{\omega}\sin\theta \\ -\sin\theta - \mathrm{i}\frac{f}{\omega}\cos\theta \\ \frac{\kappa H}{\omega} \end{pmatrix} \mathrm{d}\hat{\phi}(\boldsymbol{k},\omega), \tag{3.13}$$

$$\mathbb{E}\overline{\mathrm{d}\hat{\phi}(\boldsymbol{k},\omega)}\mathrm{d}\hat{\phi}(\boldsymbol{k}',\omega') = (2\pi)^3 E(\boldsymbol{k},\omega)\delta(\boldsymbol{k}-\boldsymbol{k}',\omega-\omega')\,\mathrm{d}k\,\mathrm{d}k'\,\mathrm{d}l\,\mathrm{d}l'\,\mathrm{d}\omega\,\mathrm{d}\omega', \tag{3.14}$$

and

$$E(\boldsymbol{k},\omega) = 2\pi\left[\delta(\omega-\omega_0(\kappa)) + \delta(\omega+\omega_0(\kappa))\right]\frac{1}{2}E(\boldsymbol{k}). \tag{3.15}$$

For a real wave field, we also have

$$\overline{\mathrm{d}\hat{\phi}(\boldsymbol{k},\omega)} = \mathrm{d}\hat{\phi}(-\boldsymbol{k},-\omega). \tag{3.16}$$

The normalization of (3.14) is chosen such that

$$\bar{E} = \frac{1}{2}\mathbb{E}\left(|u_1|^2 + |v_1|^2 + \frac{g}{H}|h_1\mathscr{L}h_1|\right) = \frac{1}{(2\pi)^3}\int E(\boldsymbol{k},\omega)\,\mathrm{d}k\,\mathrm{d}l\,\mathrm{d}\omega = \frac{1}{(2\pi)^2}\int E(\boldsymbol{k})\,\mathrm{d}k\,\mathrm{d}l.$$

Here, $\bar{E}$ is the expected value of the linear energy density per unit area. We now restrict ourselves to the case where the spectrum is isotropic, i.e.

$$E(\boldsymbol{k})\,\mathrm{d}k\,\mathrm{d}l = E(k,l)\,\mathrm{d}k\,\mathrm{d}l = S(\kappa)\,\mathrm{d}\kappa\,\mathrm{d}\theta \quad \Leftrightarrow \quad S(\kappa) = \kappa E(\kappa\cos\theta, \kappa\sin\theta), \tag{3.17}$$

where $S(\kappa)$ is a non-negative function. This implies

$$\bar{E} = \frac{1}{2\pi}\int_0^\infty S(\kappa)\,\mathrm{d}\kappa. \tag{3.18}$$

4. The second-order Lagrangian velocity

Our aim is to use (2.2) to calculate the leading-order diffusivity in a random wave field and this requires knowing the Lagrangian velocity field at sufficient accuracy. At

$O(a)$, the relevant velocity field is simply the linear wave field, but as noted before this does not lead to any diffusion if the wave frequency spectrum is bounded away from zero. This means we need to know the Lagrangian velocity field at $O(a^2)$, so we need to compute

$$\boldsymbol{u}_2^L = \boldsymbol{u}_2 + \boldsymbol{u}_2^S, \quad \text{where} \quad \boldsymbol{u}_2^S = (\boldsymbol{\xi}_1 \cdot \nabla)\boldsymbol{u}_1 \tag{4.1}$$

is the Stokes drift based on the usual linear particle displacement field $\boldsymbol{\xi}_1$ such that $\partial_t \boldsymbol{\xi}_1 = \boldsymbol{u}_1$. These standard definitions ensure that $\boldsymbol{u}_2^L(\boldsymbol{x}, t)$ captures the $O(a^2)$ velocity of the particle that performs zero-mean linear wave oscillations around the point $\boldsymbol{x}$. The leading-order diffusivity based on (4.1) then arises at $O(a^4)$.

Now, $\boldsymbol{u}_2^S$ is a wave property in the sense that it can be computed directly from the linear wave field. On the other hand, the Eulerian velocity $\boldsymbol{u}_2$ needs to be computed from the fluid equations at $O(a^2)$. This is a cumbersome procedure but substantial simplifications occur if we concentrate on the low-frequency part of $\boldsymbol{u}_2^L$ as the only part relevant for diffusion. Specifically, we will make frequent use of the result (2.7), which allows us to neglect time derivative components of $\boldsymbol{u}_2^L$. Henceforth, we will use the symbol $\stackrel{t}{=}$ to mean 'equal up to a time derivative of a stationary function'.

4.1. *Low-frequency equations*

We use a Helmholtz decomposition for $\boldsymbol{u}_2^L$ such that $\nabla \cdot \boldsymbol{u}_2^L$ and $\nabla \times \boldsymbol{u}_2^L$ are considered in turn. First, the divergence $\nabla \cdot \boldsymbol{u}_2^L = \nabla \cdot \boldsymbol{u}_2 + \nabla \cdot \boldsymbol{u}_2^S$ is determined as follows. The $O(a^2)$ continuity equation is

$$\nabla \cdot (H\boldsymbol{u}_2 + h_1\boldsymbol{u}_1) = -\partial_t h_2 \quad \Leftrightarrow \quad \nabla \cdot \boldsymbol{u}_2 \stackrel{t}{=} -\frac{1}{H}\nabla \cdot (h_1\boldsymbol{u}_1). \tag{4.2}$$

The Stokes drift by definition is

$$\boldsymbol{u}_2^S = (\boldsymbol{\xi}_1 \cdot \nabla)\boldsymbol{u}_1 = \nabla \cdot (\boldsymbol{u}_1\boldsymbol{\xi}_1) - \boldsymbol{u}_1 \nabla \cdot \boldsymbol{\xi}_1 = \nabla \cdot (\boldsymbol{u}_1\boldsymbol{\xi}_1) + \frac{h_1\boldsymbol{u}_1}{H}. \tag{4.3}$$

Here the divergence operator contracts with $\boldsymbol{\xi}_1$ and we used $H\nabla \cdot \boldsymbol{\xi}_1 = -h_1$ from the linear equations. Taking the divergence and using $\boldsymbol{\xi}_1 = (\xi, \eta)$ leads to

$$\nabla \cdot \boldsymbol{u}_2^S = \frac{\partial}{\partial t}\left(\frac{1}{2}\partial_{xx}^2\xi^2 + \frac{1}{2}\partial_{yy}^2\eta^2 + \partial_{xy}^2\xi\eta\right) + \frac{1}{H}\nabla \cdot (h_1\boldsymbol{u}_1) \stackrel{t}{=} \frac{1}{H}\nabla \cdot (h_1\boldsymbol{u}_1). \tag{4.4}$$

Adding (4.2) and (4.4) gives

$$\nabla \cdot \boldsymbol{u}_2^L \stackrel{t}{=} 0, \tag{4.5}$$

which shows that the divergence part of $\boldsymbol{u}_2^L$ does not contribute to the diffusivity. In other words, for the purpose of computing the diffusivity, we can treat $\boldsymbol{u}_2^L$ as incompressible.

Next, we determine $\nabla \times \boldsymbol{u}_2^L = \nabla \times \boldsymbol{u}_2 + \nabla \times \boldsymbol{u}_2^S$ at low frequency. Again, we first consider the Eulerian component. Taking ∂_t of the continuity equation, keeping terms of $O(a^2)$ and substituting the $O(a^2)$ PV constraint $H\nabla \times \boldsymbol{u}_2 = fh_2$ gives

$$(\nabla \times \boldsymbol{u}_2)_{tt} + f(\nabla \cdot \boldsymbol{u}_2)_t = \frac{-f}{H}\nabla \cdot (h_1\boldsymbol{u}_1)_t. \tag{4.6}$$

The term $(\nabla \cdot \boldsymbol{u}_2)_t$ can be replaced using the momentum equations and this yields

$$(\partial_{tt} - c^2\nabla^2\mathscr{L} + f^2)\nabla \times \boldsymbol{u}_2 = f\nabla^2\frac{1}{2}|\boldsymbol{u}_1|^2 - \frac{f^2}{H}\nabla \times (h_1\boldsymbol{u}_1) - \frac{f}{H}\nabla \cdot (h_1\boldsymbol{u}_1)_t. \tag{4.7}$$

Omitting time derivatives and adding the Stokes drift yields

$$(-c^2\nabla^2\mathscr{L}+f^2)\nabla\times\boldsymbol{u}_2^L \stackrel{t}{=} (-c^2\nabla^2\mathscr{L}+f^2)\nabla\times\boldsymbol{u}_2^S + f\nabla^2\frac{1}{2}|\boldsymbol{u}_1|^2 - \frac{f^2}{H}\nabla\times(h_1\boldsymbol{u}_1). \quad (4.8)$$

In the special case of a slowly varying wavetrain, $\boldsymbol{u}_2^S$ and $h_1\boldsymbol{u}_1/H$ are both equal to the pseudomomentum vector and after inverting a Laplacian the present equation reduces to (1.3) in Bühler & McIntyre (1998). For general random waves, this is not the case and we will work with (4.8) in the form

$$\nabla\times\boldsymbol{u}_2^L \stackrel{t}{=} \nabla\times\boldsymbol{u}_2^S + f(f^2-c^2\nabla^2\mathscr{L})^{-1}\left(\nabla^2\frac{1}{2}|\boldsymbol{u}_1|^2 - \frac{f}{H}\nabla\times(h_1\boldsymbol{u}_1)\right). \quad (4.9)$$

This is the central expression for $\nabla\times\boldsymbol{u}^L$ that we will use together with (4.5) to compute the diffusivity. Despite considerable effort, we did not succeed in finding a simple relation between $\boldsymbol{u}_2^L$ and the Stokes drift or perhaps the pseudomomentum of the waves, even though such relationships are readily available in the context of slowly varying wavetrains as shown by Bühler & McIntyre (1998).

In the case of no rotation, (4.9) reduces to the trivial equation

$$\nabla\times\boldsymbol{u}_2^L \stackrel{t}{=} \nabla\times\boldsymbol{u}_2^S. \quad (4.10)$$

Together with (4.5) this means that in this case the low-frequency part of $\boldsymbol{u}_2^L$ is simply the least-squares projection of $\boldsymbol{u}_2^S$ onto non-divergent vector fields. In the standard shallow-water equations with $\hat{L}=1$, it is possible to show that $\nabla\cdot(h_1\boldsymbol{u}_1)\stackrel{t}{=}0$, so, in fact, each of the Stokes and Lagrangian flows are separately non-divergent at low frequency. In this case, one could simply set $\boldsymbol{u}_2^L \stackrel{t}{=} \boldsymbol{u}_2^S$ for the computation of the diffusivity, as the divergent part of $\boldsymbol{u}_2^S$ would only add an inconsequential time derivative part. Therefore, a naive nonlinear trajectory computation based solely on the $O(a)$ wave field would lead to the correct diffusivity at $O(a^4)$. However, we will clearly see below that this is not the case if $f\neq 0$.

4.2. *Computing the correlation function for second-order fields*

The task is now to use (4.9)–(4.10) in order to compute the covariance structure of $\boldsymbol{u}_2^L$ and ultimately the diffusivity based on this velocity field. This is conceptually straightforward, but technically arduous for the following reason. To begin with, the linear wave fields are represented by a three-dimensional integral over $(\boldsymbol{k},\omega)$ in (3.11) and, therefore, the quadratic source terms (4.9), as well as $\boldsymbol{u}_2^L$ itself, are represented by a six-dimensional integral over two copies of this space. Following this reasoning, the covariance structure of $\boldsymbol{u}_2^L$ is then given by a twelve-dimensional integral and the leading-order diffusivity

$$D_{u^L} = \frac{1}{2}\int_{-\infty}^{+\infty} \mathbb{E}u_2^L(0,0,0)u_2^L(0,0,t)\,\mathrm{d}t \quad (4.11)$$

is finally given by a thirteen-dimensional integral. On the other hand, simplifications arise because $\boldsymbol{u}_2^L$ needs to be evaluated at $x=y=0$ only, the fourth moments of $\mathrm{d}\hat{\phi}$ arising in (4.11) can be reduced to second moments using the Gaussian distribution, and the time integral in (4.11) allows making frequent use of the identity

$$2\pi\,\delta(\omega) = \int_{-\infty}^{+\infty} \mathrm{e}^{\mathrm{i}\omega t}\,\mathrm{d}t. \quad (4.12)$$

As an example for what is involved, we will now compute the covariance function of the term $\nabla \times (h_1 \boldsymbol{u}_1)$ that appears in (4.9). From (3.11) and (3.13), it follows that

$$h_1 u_1 = \frac{1}{(2\pi)^6} \int H \frac{\kappa_1}{\omega_1} \left(-\cos\theta_2 + \mathrm{i} \frac{f}{\omega_2} \sin\theta_2 \right) \mathrm{e}^{\mathrm{i}\boldsymbol{X}\cdot(\boldsymbol{K}_1+\boldsymbol{K}_2)} \mathrm{d}\hat{\phi}_1 \mathrm{d}\hat{\phi}_2,$$
$$h_1 v_1 = \frac{1}{(2\pi)^6} \int H \frac{\kappa_1}{\omega_1} \left(-\sin\theta_2 - \mathrm{i} \frac{f}{\omega_2} \cos\theta_2 \right) \mathrm{e}^{\mathrm{i}\boldsymbol{X}\cdot(\boldsymbol{K}_1+\boldsymbol{K}_2)} \mathrm{d}\hat{\phi}_1 \mathrm{d}\hat{\phi}_2.$$

Here, we use the short-hands $\boldsymbol{X} = (x, y, t)$, $\boldsymbol{K} = (k, l, \omega)$ and $\mathrm{d}\hat{\phi}_{1,2} = \mathrm{d}\hat{\phi}(\boldsymbol{K}_{1,2})$. Clearly, taking an x-derivative corresponds to multiplying the integrand by $\mathrm{i}(k_1 + k_2)$ and a y-derivative to multiplying by $\mathrm{i}(l_1 + l_2)$, so

$$\nabla \times (h_1 \boldsymbol{u}_1) = \frac{H}{(2\pi)^2} \int \frac{\kappa_1}{\omega_1} \left(\mathrm{i}\kappa_1 \sin(\theta_1 - \theta_2) + \frac{f}{\omega_2} (\kappa_2 + \kappa_1 \cos(\theta_1 - \theta_2)) \right) \times \mathrm{e}^{\mathrm{i}\boldsymbol{X}\cdot(\boldsymbol{K}_1+\boldsymbol{K}_2)} \mathrm{d}\hat{\phi}_1 \mathrm{d}\hat{\phi}_2. \quad (4.13)$$

The generic definition $C_{A,A}(\boldsymbol{X}) = \mathbb{E}\overline{A(0)}A(\boldsymbol{X})$ leads to

$$C_{\nabla\times(h_1\boldsymbol{u}_1),\nabla\times(h_1\boldsymbol{u}_1)} = \frac{1}{(2\pi)^{12}} H^2 \int \frac{\kappa_1\kappa_3}{\omega_1\omega_3} \left(\mathrm{i}\kappa_1 \sin(\theta_1-\theta_2) + \frac{f}{\omega_2}(\kappa_2 + \kappa_1 \cos(\theta_1-\theta_2)) \right)$$
$$\times \left(-\mathrm{i}\kappa_3 \sin(\theta_3-\theta_4) + \frac{f}{\omega_4}(\kappa_4 + \kappa_3 \cos(\theta_3-\theta_4)) \right) \mathrm{e}^{\mathrm{i}(\boldsymbol{K}_1+\boldsymbol{K}_2)\cdot\boldsymbol{X}} \mathbb{E}\mathrm{d}\hat{\phi}_1 \mathrm{d}\hat{\phi}_2 \overline{\mathrm{d}\hat{\phi}_3 \, \mathrm{d}\hat{\phi}_4}, \quad (4.14)$$

where the index pairs (1, 2) and (3, 4) correspond to the field at $\boldsymbol{X}$ and at the origin, respectively. Since the $\mathrm{d}\phi_i$ are Gaussian measures, the fourth moment can be expressed as a sum of second moments via

$$\mathbb{E}\mathrm{d}\hat{\phi}_1 \mathrm{d}\hat{\phi}_2 \overline{\mathrm{d}\hat{\phi}_3 \, \mathrm{d}\hat{\phi}_4} = \mathbb{E}(\mathrm{d}\hat{\phi}_1 \mathrm{d}\hat{\phi}_2) \mathbb{E}(\overline{\mathrm{d}\hat{\phi}_3 \, \mathrm{d}\hat{\phi}_4}) + \mathbb{E}(\mathrm{d}\hat{\phi}_1 \overline{\mathrm{d}\hat{\phi}_3}) \mathbb{E}(\mathrm{d}\hat{\phi}_2 \overline{\mathrm{d}\hat{\phi}_4})$$
$$+ \mathbb{E}(\mathrm{d}\hat{\phi}_1 \overline{\mathrm{d}\hat{\phi}_4}) \mathbb{E}(\mathrm{d}\hat{\phi}_2 \overline{\mathrm{d}\hat{\phi}_3}).$$

The first term is zero if the field is complex, but for a real field it is

$$(2\pi)^6 E(\boldsymbol{K}_1) E(\boldsymbol{K}_3) \delta(\boldsymbol{K}_1 + \boldsymbol{K}_2) \delta(\boldsymbol{K}_3 + \boldsymbol{K}_4) \, \mathrm{d}\boldsymbol{K}_1 \, \mathrm{d}\boldsymbol{K}_2 \, \mathrm{d}\boldsymbol{K}_3 \, \mathrm{d}\boldsymbol{K}_4 \quad (4.15)$$

after using (3.14). Now, (4.15) means that only $\kappa_1 = \kappa_2$, $\kappa_3 = \kappa_4$ and $\theta_1 - \theta_2 = \theta_3 - \theta_4 = \pi$ matter in (4.14), which implies that the integrand vanishes. Therefore, the integral belonging to (4.15) is zero. Similarly, using (3.14), the second and third terms lead to

$$(2\pi)^6 E(\boldsymbol{K}_1) E(\boldsymbol{K}_2) (\delta(\boldsymbol{K}_1 - \boldsymbol{K}_3) \delta(\boldsymbol{K}_2 - \boldsymbol{K}_4) + \delta(\boldsymbol{K}_1 - \boldsymbol{K}_4) \delta(\boldsymbol{K}_2 - \boldsymbol{K}_3)) \, \mathrm{d}\boldsymbol{K}_1 \, \mathrm{d}\boldsymbol{K}_2 \, \mathrm{d}\boldsymbol{K}_3 \, \mathrm{d}\boldsymbol{K}_4.$$

Integrating (4.14) over $\boldsymbol{K}_3$ and $\boldsymbol{K}_4$ finally leads to

$$C_{\nabla\times(h_1\boldsymbol{u}_1),\nabla\times(h_1\boldsymbol{u}_1)} = \frac{1}{(2\pi)^6} H^2 \int \left(\frac{\kappa_1^2}{\omega_1^2} \left(\kappa_1^2 \sin^2(\theta_1-\theta_2) + \frac{f^2}{\omega_2^2} (\kappa_2\kappa_1 \cos(\theta_1-\theta_2))^2 \right) \right.$$
$$+ \frac{\kappa_1\kappa_2}{\omega_1\omega_2} \left(\frac{f^2}{\omega_1\omega_2} (\kappa_1 + \kappa_2 \cos(\theta_1-\theta_2))(\kappa_2 + \kappa_1 \cos(\theta_1-\theta_2)) - \kappa_1\kappa_2 \sin(\theta_1-\theta_2) \right.$$
$$\left. \left. - \mathrm{i}f \frac{\kappa_2}{\omega_2} \sin(\theta_1-\theta_2)(\kappa_2 + \kappa_1 \cos(\theta_1-\theta_2)) + \mathrm{i}f \frac{\kappa_1}{\omega_1} \sin(\theta_1-\theta_2)(\kappa_1 + \kappa_2 \cos(\theta_1-\theta_2)) \right) \right)$$
$$\times \mathrm{e}^{\mathrm{i}(\boldsymbol{K}_1+\boldsymbol{K}_2)\cdot\boldsymbol{X}} E(\boldsymbol{K}_1) E(\boldsymbol{K}_2) \, \mathrm{d}\boldsymbol{K}_1 \, \mathrm{d}\boldsymbol{K}_2. \quad (4.16)$$

Because of the crucial Gaussianity assumption for the wave fields, this covariance function is given by an integral over six dimensions rather than twelve.

4.3. *Leading-order diffusivity*

We can now turn to computing the leading-order diffusivity. The algebra is even less forgiving than in the previous section, so we will only outline the procedure and state the results, relegating more details to the Appendix. First off, since $\nabla\cdot\boldsymbol{u}_2^L \overset{t}{=} 0$, there is a random streamfunction ψ such that $\boldsymbol{u}_2^L \overset{t}{=} (-\psi_y, \psi_x)$ and $\nabla\times\boldsymbol{u}_2^L = \nabla^2\psi$. We find it convenient to compute ψ such that $C_{u_2^L,u_2^L} = -\frac{\partial^2}{\partial y^2}C_{\psi,\psi}$, $C_{v_2^L,v_2^L} = -\frac{\partial^2}{\partial x^2}C_{\psi,\psi}$, where $C_{\psi,\psi}(x,y,t)$ is the covariance function of ψ at the space–time lags (x,y,t). We will compute this function and then use the symmetrized expression

$$D_{u_2^L} + D_{v_2^L} = 2D = \frac{1}{2}\int_{-\infty}^{\infty} -\nabla^2 C_{\psi,\psi}(x=0,\, y=0,\, t)\,\mathrm{d}t \tag{4.17}$$

for the one-particle diffusivity D based on an isotropic spectrum. We use (4.9) to solve for ψ in Fourier space and thus obtain an expression for ψ in terms of a six-dimensional integral as in (4.13). Let us write the integrand as $\gamma(\boldsymbol{K}_1, \boldsymbol{K}_2)$ so that

$$\psi = \frac{1}{(2\pi)^6}\int \gamma(\boldsymbol{K}_1, \boldsymbol{K}_2)\mathrm{e}^{\mathrm{i}\boldsymbol{X}\cdot(\boldsymbol{K}_1+\boldsymbol{K}_2)}\mathrm{d}\hat{\phi}_1\mathrm{d}\hat{\phi}_2\,. \tag{4.18}$$

The exact form of γ is given in § A.1. Retracing the steps that led to (4.16), we first obtain

$$C_{\psi,\psi}(\boldsymbol{X}) = \frac{1}{(2\pi)^{12}}\int \gamma(\boldsymbol{K}_1, \boldsymbol{K}_2)\overline{\gamma(\boldsymbol{K}_3, \boldsymbol{K}_4)}\mathrm{e}^{\mathrm{i}(\boldsymbol{K}_1+\boldsymbol{K}_2)\cdot\boldsymbol{X}}\mathbb{E}\mathrm{d}\hat{\phi}_1\mathrm{d}\hat{\phi}_2\overline{\mathrm{d}\hat{\phi}_3\,\mathrm{d}\hat{\phi}_4}.$$

and eventually

$$C_{\psi,\psi} = \frac{1}{(2\pi)^6}\int (|\gamma(\boldsymbol{K}_1, \boldsymbol{K}_2)|^2 + \gamma(\boldsymbol{K}_1, \boldsymbol{K}_2)\overline{\gamma(\boldsymbol{K}_2, \boldsymbol{K}_1)})E(\boldsymbol{K}_1)E(\boldsymbol{K}_2)\mathrm{e}^{\mathrm{i}(\boldsymbol{K}_1+\boldsymbol{K}_2)\cdot\boldsymbol{X}}\,\mathrm{d}\boldsymbol{K}_1\,\mathrm{d}\boldsymbol{K}_2.$$

This integral is symmetric if the variable labels (1, 2) are interchanged, and averaging over the two possible label sets yields an integrand that is explicitly symmetric and easier to deal with. Finally, we take $-\nabla^2$ (by multiplying the integrand by $(k_1+k_2)^2+(l_1+l_2)^2$) to get

$$-\nabla^2 C_{\psi,\psi}(\boldsymbol{X}) = \frac{1}{(2\pi)^6}\int g(\boldsymbol{K}_1, \boldsymbol{K}_2)E(\boldsymbol{K}_1)E(\boldsymbol{K}_2)\mathrm{e}^{\mathrm{i}(\boldsymbol{K}_1+\boldsymbol{K}_2)\cdot\boldsymbol{X}}\,\mathrm{d}\boldsymbol{K}_1\,\mathrm{d}\boldsymbol{K}_2, \tag{4.19}$$

where $g(\boldsymbol{K}_1, \boldsymbol{K}_2) = \frac{1}{2}|\gamma(\boldsymbol{K}_1, \boldsymbol{K}_2)+\gamma(\boldsymbol{K}_2, \boldsymbol{K}_1)|^2(\kappa_1^2+\kappa_2^2+2\kappa_1\kappa_2\cos(\theta_1-\theta_2))$ is symmetric in each of its three pairs of arguments. We now substitute $x=y=0$, change to polar variables, integrate over θ_1, θ_2 (which we can do without knowing the exact form of the energy spectrum or dispersion relation, since these were assumed to be isotropic) and integrate over ω_1, ω_2 by using the delta functions in (3.15). The non-trivial step in this recipe is the integration of $g(\boldsymbol{K}_1, \boldsymbol{K}_2)$ over the angles, which is described in § A.1 in the Appendix. The result is

$$\begin{aligned}-\nabla^2 C_{\psi,\psi}(0,0,t) = \frac{1}{(2\pi)^2}\int \frac{1}{4}\{&g(\kappa_1, \omega_1, \kappa_2, \omega_2)\mathrm{e}^{\mathrm{i}(\omega_1+\omega_2)t} + g(\kappa_1, \omega_1, \kappa_2, -\omega_2)\mathrm{e}^{\mathrm{i}(\omega_1-\omega_2)t}\\ &+ g(\kappa_1, -\omega_1, \kappa_2, -\omega_2)\mathrm{e}^{-\mathrm{i}(\omega_1+\omega_2)t} + g(\kappa_1, -\omega_1, \kappa_2, \omega_2)\mathrm{e}^{-\mathrm{i}(\omega_1-\omega_2)t}\}\\ &\times S(\kappa_1)S(\kappa_2)\,\mathrm{d}\kappa_1\,\mathrm{d}\kappa_2,\end{aligned} \tag{4.20}$$

where we use (3.18) and the short-hand $\omega_i = \omega_0(\kappa_i) \geqslant f$. Here, the function g is

$$g(\kappa_1, \omega_1, \kappa_2, \omega_2) = \frac{1}{(2\pi)^2} \int g(\boldsymbol{K}_1, \boldsymbol{K}_2)\, \mathrm{d}\theta_1\, \mathrm{d}\theta_2 = \frac{1}{2\pi} \int g(\boldsymbol{K}_1, \boldsymbol{K}_2)\, \mathrm{d}(\theta_1 - \theta_2), \quad (4.21)$$

which works because $g(\boldsymbol{K}_1, \boldsymbol{K}_2)$ depends only on $\theta_1 - \theta_2$. We are now ready to evaluate (4.17) using (4.20) and the identity (4.12), which turns the time-dependent factors $\exp(\mathrm{i}(\omega_1 \pm \omega_2)t)$ into $2\pi\delta(\omega_1 \pm \omega_2)$. The frequency function is non-negative by definition, and by assumption we are not allowing waves at zero frequency, so only the $\delta(\omega_1 - \omega_2)$ terms matter, which, by the isotropic dispersion relation, implies that the only relevant wavenumber locations in (4.20) are $\kappa_1 = \kappa_2$. Performing the integral over κ_2 whilst noting the scaling properties of the delta function leads to

$$2D = \frac{1}{2\pi} \int \frac{1}{2} g(\kappa, \omega_0(\kappa), \kappa, -\omega_0(\kappa))\, S(\kappa)^2\, \frac{\mathrm{d}\kappa}{|\omega_0'(\kappa)|}, \quad (4.22)$$

where we replaced κ_1 by κ, reinstated the dispersion relation and combined two identical terms because g is symmetric. Let us pull out the part of the integrand that does not depend on the unknown energy spectrum by defining

$$G(\kappa) \equiv g(\kappa, \omega_0(\kappa), \kappa, -\omega_0(\kappa)) \frac{c^3}{|\omega_0'(\kappa)|}, \quad (4.23)$$

so that the diffusivity is

$$2D = \frac{1}{2\pi c^3} \frac{1}{2} \int G(\kappa) S(\kappa)^2\, \mathrm{d}\kappa. \quad (4.24)$$

The non-dimensional function $G(\kappa)$ can be thought of as a kind of diffusivity density in spectral space. In the next section, we examine this function more closely.

5. Analysis of diffusivity density

The diffusivity density $G(\kappa)$ tells us how effective are waves at different scales at generating single-particle dispersion. We will see that this depends crucially on the strength of the rotation. Before going into specifics, we can note two general consequences of the form of (4.24) and the fact that $G(\kappa) \geqslant 0$ (see the Appendix). First, the net diffusivity D can be viewed as a sum over positive definite contributions from different wavenumbers κ, i.e. adding more wave energy at any scale always increases D. Second, because the diffusivity is proportional to the spectral wave energy squared, there is a divergence of D if a finite amount of wave energy $\bar{E}$ is confined to an infinitesimal ring in wavenumber space such that $S \neq 0$ only in a neighbourhood of size $\Delta\kappa$ around some central value κ_0, say. In this case

$$\bar{E} \propto S(\kappa_0)\, \Delta\kappa \quad \Rightarrow \quad D \propto G(\kappa_0) \frac{\bar{E}^2}{\Delta\kappa}, \quad (5.1)$$

which diverges as $\Delta\kappa \to 0$. Presumably, the physical interpretation of this divergence is that in this limit the frequency bandwidth $\Delta\omega \to 0$ as well and, therefore, the auto-correlation time of the wave field diverges and so does D based on (2.5).

5.1. *The influence of rotation*

From here onwards, we use the standard shallow-water dispersion relation by setting $\hat{L} = 1$. Using the non-dimensional variable

$$n = \frac{\kappa c}{f} \quad (5.2)$$

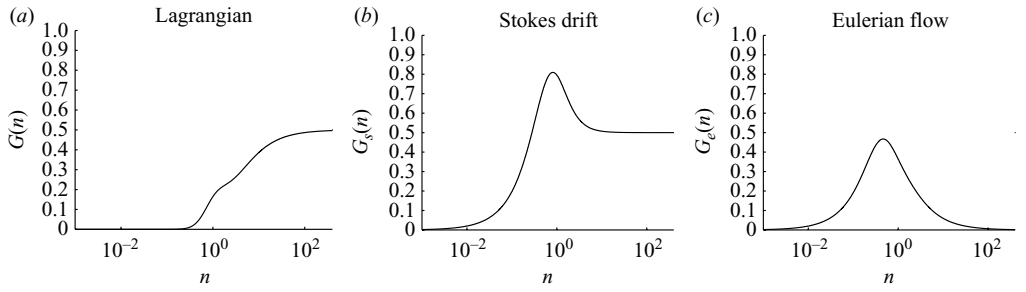

FIGURE 1. Spectral diffusivity density $G(n)$ given in (5.3) (a). Diffusivity densities $G_s(n)$, $G_e(n)$ induced by the Stokes drift (b) and Eulerian flow (c). A logarithmic scale is used for n.

the exact analytic expression for $G(n)$ as derived in the Appendix is

$$G(n) = \frac{1}{12}\sqrt{\frac{n^2+1}{n^2}}\left(6 - \frac{6}{(1+n^2)^3} - \frac{12}{(1+n^2)^2} + \frac{27}{1+n^2} - \frac{3}{(1+4n^2)^{3/2}} + \frac{11}{\sqrt{1+4n^2}} - \frac{12\sqrt{1+4n^2}}{(1+n^2)^2} - \frac{11\sqrt{1+4n^2}}{1+n^2}\right). \quad (5.3)$$

This is our central theoretical result and it is plotted in figure 1. The non-rotating case $f = 0$ corresponds to $n \to \infty$, which gives the limit $G = 1/2$, so in this case no spatial scale is preferred and

$$f = 0: \quad D = \frac{1}{2\pi c^3}\frac{1}{8}\int S(\kappa)^2 \,\mathrm{d}\kappa. \quad (5.4)$$

Hence, if $f = 0$ then the diffusivity is simply a constant times the $\mathbb{L}_2$-norm of the energy spectrum, which is a result that could perhaps have been guessed by dimensional analysis. It implies, for instance, that any energy-conserving spreading of wave energy due to weakly nonlinear wave–wave interactions would tend to decrease D.

Now, as indicated by figure 1, the function $G(n)$ increases monotonically with n. Specifically, below $n = O(1)$ the function decays rapidly with n and eventually goes to zero as n^5. Physically, the diffusivity density is strongest on scales far smaller than the deformation scale c/f and it is negligible at scales far larger than the deformation scale. Also, the diffusivity at any wavenumber κ decreases if the rotation f increases, as this decreases the effective n. We do not find this monotonic behaviour an intuitively obvious fact. For instance, increasing f at fixed κ *increases* the relative share of kinetic energy of inertia–gravity waves, which would suggest that 'more' particle motion per unit energy is taking place as f is increased.

In an effort to understand the structure of $G(n)$, we decompose the Lagrangian flow into the sum of a Stokes drift $\boldsymbol{u}_2^S$ and an Eulerian flow $\boldsymbol{u}_2$ and compute the diffusivity density induced by each of these flow components separately. We will call these diffusivity densities $G_s(n)$ and $G_e(n)$, respectively. The full Lagrangian diffusivity will be the sum of these two diffusivity densities plus a cross-correlation term, i.e. $G \neq G_s + G_e$. The exact analytic expressions are

$$G_s(n) = \frac{n}{2}\frac{(2+n^2)^2}{(1+n^2)^{5/2}} \quad (5.5)$$

and

$$G_e(n) = \frac{-1 + 20n^6 + \sqrt{1+4n^2} - 4n^2(-6+\sqrt{1+4n^2}) + 3n^2(1+\sqrt{1+4n^2})}{4(1+n^2)^{3/2}(1+4n^2)^{3/2}n}. \quad (5.6)$$

These are plotted in figure 1. The Stokes drift diffusivity density $G_s(n)$ increases with n to a peak near $n = 1$ and then decays slightly and converges to $1/2$ as $n \to \infty$. The Eulerian flow diffusivity density $G_e(n)$ also increases to a sharp peak near $n = 0.5$ and then decays to 0. Since the Lagrangian diffusivity increases monotonically, we can infer that the two components are strongly anti-correlated when $n = O(1)$ or below. Indeed, both (5.5) and (5.6) have the limiting form $2n$ as $n \to 0$, which is much stronger than the Lagrangian diffusivity, which is $7n^5$ in the same limit. This makes obvious the fact that for strong rotation both the Stokes drift and the Eulerian flow grossly overestimate the Lagrangian diffusivity. This can be traced back to a near-cancellation of Stokes drift and Eulerian flow, which leads to the choking of the Lagrangian flow.

5.2. *A scaling argument for strong rotation*

Here, we provide a scaling argument for D in the limit of strong rotation, where the Lagrangian flow appears to be peculiarly weak. For this, we consider a narrow-band spectrum with width $\Delta\kappa$ centred at some wavenumber κ_0 such that $\Delta\kappa \ll \kappa_0$ and $N = \kappa_0 c/f \ll 1$. We view changing N as a simile for changing f, although we could achieve the same scalings by varying c. Inspired by (2.5), we will estimate D by finding scalings for $\mathbb{E}|\boldsymbol{u}_2^L|^2$ and τ_u separately in the limit $N \to 0$. There is some ambiguity because, as discussed before, we can add the time derivative of any stationary random function to $\boldsymbol{u}_2^L$ without changing D, but doing so does change the variance $\mathbb{E}|\boldsymbol{u}_2^L|^2$ and the correlation time τ_u separately. Still, we have found that if the obvious time-derivative terms are subtracted, then the correlation time for all three fields $(\boldsymbol{u}_2^L, \boldsymbol{u}_2^S, \boldsymbol{u}_2)$ is equal and simply proportional to the inverse of the frequency bandwidth of the wave spectrum: $\tau_u \propto 1/\Delta\omega$. With the approximation $\Delta\omega \approx \Delta\kappa(c^2\kappa_0/f)$ from the dispersion relation for small N, this gives

$$\tau_u \sim \frac{1}{c\Delta\kappa N} \propto f. \quad (5.7)$$

Thus, the correlation time grows linearly with f in the limit of strong rotation.

Now, to obtain a scaling for $\mathbb{E}|\boldsymbol{u}_2^L|^2$, we consider a non-dimensional version of (4.9) where we use (f, κ_0) as time and space scales and U as a wave velocity scale such that $U^2 \propto \bar{E}$. The aim is to determine U^L, the relevant scale for $\boldsymbol{u}_2^L$ as $N \to 0$. The non-dimensional (4.9) is

$$\frac{U^L c}{U^2 N}\nabla \times \boldsymbol{u}_2^L \stackrel{t}{=} \nabla \times \boldsymbol{u}_2^S + (1 - N^2\nabla^2)^{-1}\left(\frac{1}{2}\nabla^2|\boldsymbol{u}_1|^2 - \nabla \times (h_1 \boldsymbol{u}_1)\right). \quad (5.8)$$

We can rewrite this equation by removing some terms from the right-hand side that are time-derivatives (see § A.2 in the Appendix). The result is

$$\frac{U^L c}{U^2 N}\nabla \times \boldsymbol{u}_2^L \stackrel{t}{=} \nabla \times \boldsymbol{u}_2^S + (1 - N^2\nabla^2)^{-1}\left(\frac{1}{2}N^2\nabla^2(\boldsymbol{\xi}_1 \cdot \nabla h_1) - \nabla \times \boldsymbol{u}_2^S\right). \quad (5.9)$$

As $N \to 0$, the leading-order balance is

$$\frac{U^L c}{U^2 N}\nabla \times \boldsymbol{u}_2^L \stackrel{t}{=} N^2\nabla^2\left(\frac{1}{2}(\boldsymbol{\xi}_1 \cdot \nabla h_1) - \nabla \times \boldsymbol{u}_2^S\right). \quad (5.10)$$

This suggests the scaling

$$U^L \sim \frac{U^2}{c} N^3 = \frac{\bar{E}}{c} N^3 \propto f^{-3} \tag{5.11}$$

as $N \to 0$, which indeed shows a sharp decrease in the expected size of $\boldsymbol{u}_2^L$. Combining this with (5.7) yields

$$D \sim (U^L)^2 \tau_u \sim \frac{\bar{E}^2}{c^3 \Delta\kappa} N^5 \propto f^{-5},$$

in accordance with the limit of (5.3) as $n \to 0$. On the other hand, we can perform a similar analysis on the Stokes drift and the second-order Eulerian flow. A straightforward non-dimensionalization of the quadratic quantities leads to the scalings $U^s \sim U^e \sim (U^2/c)N$, which shows a much more shallow decrease than $U^L \sim N^3$. Using the same correlation time τ_u gives a scaling $D \sim N \propto 1/f$ for the diffusivity based on either of these two fields, which is again in accordance with (5.5) and (5.6). The conclusion remains clear: in the limit of strong rotation, the Stokes drift grossly overestimates the true particle dispersion.

6. Monte Carlo simulations

Monte Carlo simulations were performed to test the theoretical predictions of diffusivity. We use Fourier transforms over the spatial coordinates to compute a random initial condition for the wave variables and then we step the process forward in time by using the linear wave propagation operator to calculate the process at subsequent times. Since there are two possible values of ω for each pair (k, l), we must generate two independent random fields and step each field forward in time separately. Specifically, we use a version of (3.13) in which

$$\mathrm{d}\hat{\phi}(\boldsymbol{k}, \omega) = 2\pi\delta(\omega - \omega_0(\boldsymbol{k}))\, \mathrm{d}\hat{\phi}_1(\boldsymbol{k}) + 2\pi\delta(\omega + \omega_0(\boldsymbol{k}))\, \mathrm{d}\hat{\phi}_2(\boldsymbol{k}) \tag{6.1}$$

and the two independent measures $\mathrm{d}\hat{\phi}_{1,2}(\boldsymbol{k})$ are related to the power spectrum by

$$\mathbb{E}|\mathrm{d}\hat{\phi}_1(\boldsymbol{k})|^2 = \mathbb{E}|\mathrm{d}\hat{\phi}_2(\boldsymbol{k})|^2 = (2\pi)^2 \frac{E(\boldsymbol{k})}{2}\, \mathrm{d}k\, \mathrm{d}l. \tag{6.2}$$

The spatial domain was chosen to be periodic in x and y, with sides of length $L_x = L_y = 1500$ and $N_x = N_y = 128$ grid points were used to represent the process in space. The discretized version of (3.11)–(3.13) follows in a straightforward way by formally substituting $\Delta k \leftrightarrow \mathrm{d}k$, $\Delta l \leftrightarrow \mathrm{d}l$, $\Delta\phi \leftrightarrow \mathrm{d}\hat{\phi}$, and $\Sigma \leftrightarrow \int$ where the summation elements are

$$\Delta k = \frac{2\pi}{L_x}, \qquad \Delta l = \frac{2\pi}{L_y}. \tag{6.3}$$

The stochastic measure $\mathrm{d}\hat{\phi}$ becomes a random variable $\Delta\phi$ that by (6.1) is broken up into two separate pieces: for one we let $\Delta\phi = \Delta\phi_1$, where $\Delta\phi_1$ is associated with the branch $\omega = \omega_0$, and for the other we let $\Delta\phi = \Delta\phi_2$, where $\Delta\phi_2$ is associated with the branch $\omega = -\omega_0$. The values of these random variables depend on the grid point in question. We will index them with superscripts m, n, so that at each point (k_m, l_n) in

Fourier space, they can be generated in a manner consistent with (6.2) via

$$\Delta\phi_1^{m,n} = \sqrt{(2\pi)^2 \frac{E(k_m, l_n)}{2} \Delta k \Delta l}\, \frac{1}{\sqrt{2}} \left(A_1^{m,n} + \mathrm{i} B_1^{m,n}\right),$$

$$\Delta\phi_2^{m,n} = \sqrt{(2\pi)^2 \frac{E(k_m, l_n)}{2} \Delta k \Delta l}\, \frac{1}{\sqrt{2}} \left(A_2^{m,n} + \mathrm{i} B_2^{m,n}\right),$$

where $A_j^{m,n}$, $B_j^{m,n}$ are independent $\mathcal{N}(0, 1)$ random variables.

For a given value of t, the Gaussian random field in real space is calculated by setting $\Delta\phi_1^{m,n}(t) = \mathrm{e}^{\mathrm{i}\omega_0(\kappa_{m,n})t} \Delta\phi_1^{m,n}$, $\Delta\phi_2^{m,n}(t) = \mathrm{e}^{-\mathrm{i}\omega_0(\kappa_{m,n})t} \Delta\phi_2^{m,n}$, and calculating separate wave variables for each branch of the dispersion relation using (3.13). For example, we would compute independent fields $(\Delta\hat{u}_1^{m,n}(t), \Delta\hat{v}_1^{m,n}(t), \Delta\hat{h}_1^{m,n}(t))$ for the positive branch and $(\Delta\hat{u}_2^{m,n}(t), \Delta\hat{v}_2^{m,n}(t), \Delta\hat{h}_2^{m,n}(t))$ for the negative branch. Derivatives and anti-derivatives of wave variables are obtained by multiplication or division in Fourier space. Then, we form the sum of the branches, take the inverse two-dimensional Fourier transform of each variable and finally take the real parts of each of the resulting variables and multiply by $\sqrt{2}$. This last step is an easy way to enforce the condition (3.16).

As an example, the variable $\xi = \int u \, \mathrm{d}t$ at the spatial grid point (x, y) and time t would be calculated as

$$\xi(x, y, t) = \sqrt{2} Re \left\{ \frac{1}{(2\pi)^2} \sum_{m,n} \left[\frac{1}{\mathrm{i}\omega_0^{m,n}} \left(-\cos\theta^{m,n} + \mathrm{i} \frac{f}{\omega_0^{m,n}} \sin\theta^{m,n} \right) \Delta\phi_1^{m,n}(t) \right.\right.$$

$$\left.\left. + \frac{1}{-\mathrm{i}\omega_0^{m,n}} \left(-\cos\theta^{m,n} - \mathrm{i} \frac{f}{\omega_0^{m,n}} \sin\theta^{m,n} \right) \Delta\phi_2^{m,n}(t) \right] \mathrm{e}^{\mathrm{i}(x k_m + y l_n)} \right\}.$$

Once we have all of the desired wave variables, we can calculate the Lagrangian velocity by forming the quadratic wave quantities that appear in (4.9), and solving for $\boldsymbol{u}^L$ in Fourier space, assuming $\nabla \cdot \boldsymbol{u}^L = 0$. We did this at a finite set of times (t_i) and calculated the time-correlation functions of u^L, v^L at each fixed point in space. By taking an average over space, we obtain an estimate of the true time-correlation function. By the law of large numbers, this estimation becomes sharper as we repeat the above process and average over an increasing number of independent samples.

6.1. *One-particle diffusivity*

We used the same isotropic power spectrum for all the simulations, namely a spectrum that is non-zero only between two cut-off wavenumbers such that

$$S(\kappa) = \frac{(2\pi)^2}{\sqrt{2}} \kappa 1_{(\kappa_a, \kappa_b)} \tag{6.4}$$

in (3.17). We let $c = 1$, $\hat{L} = 1$ and varied the Coriolis parameter f. Therefore, by defining the dominant wave scale to be $\kappa_0 = (\kappa_a + \kappa_b)/2$, we could look at the diffusivity and other quantities as a function of the non-dimensional parameter $N = \kappa_0 c / f$. The cut-off wavenumbers were chosen as $(\kappa_a, \kappa_b) = (0.09, 0.12)$, which meant that roughly 25 wavelengths fit into the domain.

Figure 2 plots the results and shows very good agreement with the theoretical values calculated by integrating (4.24). As an aside, in the case $f = 0$ we also performed some direct numerical simulations in which particles were advected nonlinearly by the linear wave velocities. This procedure captures the dispersion due to the $O(a^2)$ Stokes drift, which in this non-rotating case agrees with the actual dispersion. Again,

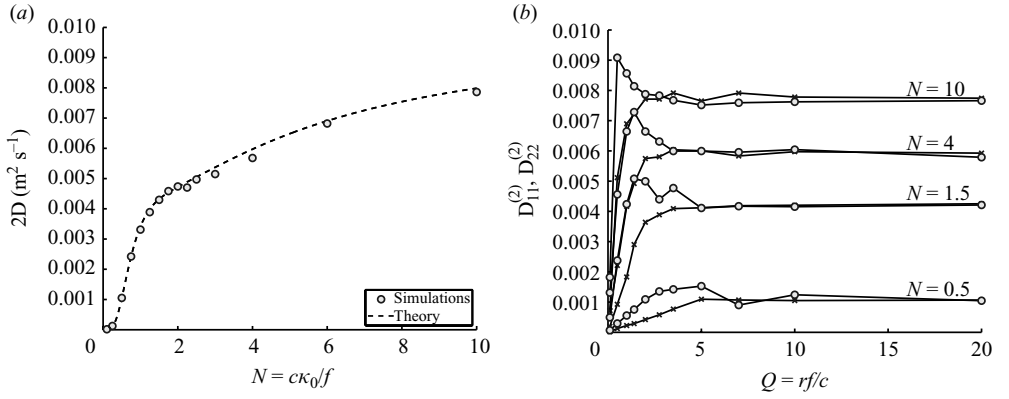

FIGURE 2. (*a*) Twice the one-particle diffusivity as a function of $N = \kappa_0 c/f$. Ten independent samples were used to estimate each point. For the chosen spectrum, the curve asymptotes towards 0.01 as $N \to \infty$. (*b*) Two-particle diffusivity as a function of non-dimensional separation Q. Each line corresponds to a different value of N, stars correspond to $D_{11}^{(2)}$ and circles correspond to $D_{22}^{(2)}$.

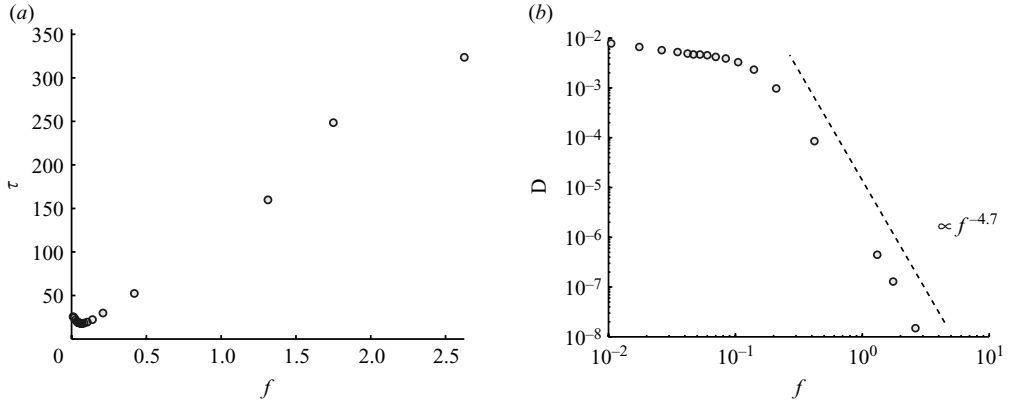

FIGURE 3. (*a*) Correlation time τ as a function of f. A linear scaling for large f is clearly visible. (*b*) D as a function of f on a log–log scale. The best-fit line for the last five data points is shifted and plotted as a dashed line. It has a slope of 4.7.

the numerical result for D in this case agreed with the theoretical prediction, and together with figure 2 this gives us significant confidence that (4.24) is indeed correct.

To test the scalings for high f in § 5.2, variables were generated using a dimensional version of (5.9). Figure 3(*a*) plots the numerical correlation time versus f. A clear linear scaling is visible, justifying our estimation of $\tau_u \sim f$. In figure 3(*b*), we plot D versus f on a log–log scale. Here, the best-fit line has a slope of -4.7, which is quite close to the estimated value of -5.

6.2. *Two-particle diffusivity*

The Monte Carlo simulations also allow us to compute the two-particle diffusivity, for which we have no analytic formula. For an isotropic system, the two-particle diffusivity $D_{ij}^{(2)}$ as defined in (2.6) has the form

$$D_{ij}^{(2)}(r_k) = A(r)\delta_{ij} + B(r)\hat{r}_i\hat{r}_j, \tag{6.5}$$

where $\hat{r}_i$ is the unit vector in the direction of the initial particle separation vector r_i and $r \geqslant 0$ is the corresponding magnitude such that $r_i = r\hat{r}_i$. We set $r_i = (r, 0)$ without loss of generality and then the functions A and B can be found from

$$D_{11}^{(2)} = A(r) + B(r) \quad \text{and} \quad D_{22}^{(2)} = A(r). \tag{6.6}$$

These components are computed using

$$D_{11}^{(2)} = \int_0^\infty \left(2C_{u_2^L,u_2^L}(0,0,\tau) - C_{u_2^L,u_2^L}(r,0,\tau) - C_{u_2^L,u_2^L}(-r,0,\tau)\right) \mathrm{d}\tau \tag{6.7}$$

and an analogous equation for $D_{22}^{(2)}$ with v_2^L replacing u_2^L. The result is plotted in figure 2 as a function of the non-dimensional separation parameter $Q = rf/c$. These plots indicate that the longitudinal diffusivity $D_{11}^{(2)}$ is less than the transversal diffusivity $D_{22}^{(2)}$ for moderate initial separations (compared with the Rossby deformation scale), and that both diffusivities eventually converge to twice the one-particle diffusivity of figure 2 in the limit of large Q. Broadly speaking, the discrepancies between the longitudinal and transversal diffusivities appear to be more pronounced for weak rotation, i.e. for large N.

7. Concluding comments

We have computed the leading-order wave-induced effective diffusivity for particle dispersion in the rotating shallow-water system. Under the assumption of a non-zero lower bound on the wave frequencies, this leading-order diffusivity is $O(a^4)$ if the waves are $O(a)$ in the wave amplitude $a \ll 1$. We derived a closed-form analytical expression for the diffusivity density in spectral space and tested the wavenumber dependence of this density using numerical Monte Carlo simulations and direct numerical simulations in the limiting case of zero rotation. Based on this, we are quite confident that our computation is correct, despite the somewhat daunting algebraic details.

As noted before, we have no simple physical explanation for the observed fact that the diffusivity due to waves at any wavenumber always decreases if the rotation is increased. Moreover, the central equation (4.9), which governs the low-frequency part of $\boldsymbol{u}_2^L$, does not seem to fit into the framework of non-dissipative wave–mean interactions developed for slowly varying wavetrains by Bühler & McIntyre (1998). Specifically, there it was possible to describe the $O(a^2)$ mean flow through a PV-inversion problem in which the waves' pseudomomentum and energy provided the effective PV. In the present case of Gaussian random waves, this does not seem to be the case, which is why we did not use the pseudomomentum in this paper. It appears that in the three-dimensional rotating Boussinesq equations, it is once again possible to obtain $\boldsymbol{u}_2^L$ via a PV-inversion problem based on pseudomomentum. Hence, it seems that the particular complications of the present shallow-water case are caused in some essential way by the apparent compressibility of the two-dimensional shallow-water fluid.

There is another interesting detail which is relevant for the oceanographic application to horizontal dispersion that motivated the present study. Namely, there is an explicit factor that diverges as the group velocity goes to zero in the equation for the diffusivity density G in (4.23). In shallow water, this happens only if $\kappa = 0$, in which case the interaction term g itself goes to zero quickly enough to not cause any problem. It appears that in the three-dimensional equation for the diffusivity that is analogous to (4.23), there is also a similar divergent factor. However, in the

three-dimensional case, it now appears that the vanishing of the group velocity as ω goes to its upper limit provides a non-trivial divergence of the diffusivity, at least in the often-studied case in which the internal wave spectrum is described by a separable power spectrum in ω and vertical wavenumber. This is ongoing work on which we hope to report shortly.

We thank Raffaele Ferrari for sharing with us an unpublished manuscript on a similar problem. Kelly Sielert performed and analysed some numerical simulations of particle trajectories as part of an undergraduate research experience. Financial support for this work under the United States National Science Foundation grant DMS-0604519 is gratefully acknowledged. M. H. C. is supported in part by a Canadian NSERC PGS-D scholarship.

Appendix

A.1. *Quantities*

The wave function for ψ, from (4.18), is

$$\begin{aligned}\gamma(\boldsymbol{K}_1, \boldsymbol{K}_2) = \frac{1}{\kappa_1^2+\kappa_2^2+2\kappa_1\kappa_2\cos(\theta_1-\theta_2)}\Bigg\{ & \mathrm{i}\frac{\kappa_2}{\omega_1}\left(\kappa_1\sin(\theta_1-\theta_2) - \mathrm{i}\frac{f}{\omega_2}(\kappa_2+\kappa_1\cos(\theta_1-\theta_2))\right) \\ & \times\left(-\cos(\theta_1-\theta_2) + \mathrm{i}\frac{f}{\omega_1}\sin(\theta_1-\theta_2)\right) + \frac{f}{f^2+\kappa_1^2+\kappa_2^2+2\kappa_1\kappa_2\cos(\theta_1-\theta_2)} \\ & \times\left(\frac{1}{2}\left[\left(\kappa_1^2+\kappa_2^2+2\kappa_1\kappa_2\cos(\theta_1-\theta_2)\right)\left(\left(1-\frac{f^2}{\omega_1\omega_2}\right)\cos(\theta_1-\theta_2)+\mathrm{i}f\right.\right.\right. \\ & \left.\left.\left.\times\left(\frac{1}{\omega_2}-\frac{1}{\omega_2}\right)\sin(\theta_1-\theta_2)\right)\right] - \mathrm{i}\frac{f\kappa_1}{\omega_1}\left[\kappa_1\sin(\theta_1-\theta_2) - \mathrm{i}\frac{f}{\omega_2}(\kappa_2+\kappa_1\cos(\theta_1-\theta_2))\right]\right)\Bigg\}.\end{aligned} \tag{A 1}$$

When $f = 0$, this reduces to

$$\gamma(\boldsymbol{K}_1, \boldsymbol{K}_2) = \frac{-\mathrm{i}\dfrac{\kappa_1\kappa_2}{\omega_1}\cos(\theta_1-\theta_2)\sin(\theta_1-\theta_2)}{\kappa_1^2+\kappa_2^2+2\kappa_1\kappa_2\cos(\theta_1-\theta_2)}.$$

Let us continue with the special case $f = 0$ to show the algebra involved in computing the diffusivity density.

The wave interaction function is

$$g(\boldsymbol{K}_1, \boldsymbol{K}_2) = \frac{1}{2}\frac{\kappa_1^2\kappa_2^2\cos^2(\theta_1-\theta_2)\sin^2(\theta_1-\theta_2)}{\kappa_1^2+\kappa_2^2+2\kappa_1\kappa_2\cos(\theta_1-\theta_2)}\left(\frac{1}{\omega_1}-\frac{1}{\omega_2}\right)^2.$$

The next two steps in the computation as described in the text are: (i) integrate over θ_1, θ_2; (ii) substitute $\kappa_1 = \kappa_2 = \kappa$ and $\omega_1 = -\omega_2 = \omega$. In fact, these operations commute, since we could just as easily have integrated out the ω_1, ω_2-dependencies before integrating out the θ_1, θ_2-dependencies. In practice, it is easier to do the computations in the reverse order, and we will do so here.

Making the substitutions (ii) yields

$$g(\kappa, \theta_1, \omega, \kappa, \theta_2, -\omega) = \frac{\kappa^2\cos^2(\theta_1-\theta_2)\sin^2(\theta_1-\theta_2)}{\omega^2(1+\cos(\theta_1-\theta_2))}.$$

The factor $1+\cos(\theta_1-\theta_2)$ from the Laplacian on the bottom cancels with part of the $\sin^2(\theta_1-\theta_2)$ factor on top, after which it is very easy to integrate over θ_1, θ_2 to get

$$g(\kappa, \omega, \kappa, -\omega) = \frac{1}{2}\frac{\kappa^2}{\omega^2}.$$

Therefore, the diffusivity density is

$$G(\kappa) = c^3 g(\kappa, \omega, \kappa, -\omega)\frac{\mathrm{d}\kappa}{\mathrm{d}\omega} = \frac{1}{2}$$

after using the dispersion relation $\omega = c\kappa$.

The algebra for computing the full diffusivity density when $f \neq 0$ is much more involved. While the cosine dependence of the Laplacian operator in the denominator cancels with factors in the numerator, as it did in the non-rotating case, the cosine dependence of the Helmholtz operator does not cancel, so the integrals over θ_1, θ_2 are more complicated. Luckily, indefinite integrals of the form $\int_\theta \cos^p\theta/(a+b\cos\theta)\,\mathrm{d}\theta$ and $\int_\theta \cos^p\theta/(a+b\cos\theta)^2\,\mathrm{d}\theta$, where p is a non-negative integer, are possible to compute analytically. Provided $a \neq b$ (a condition which is satisfied in our case when $f > 0$), the definite integrals from 0 to 2π are algebraic functions of a and b. We can use these known integrals to get an algebraic expression for $g(\kappa, \omega, \kappa, -\omega)$ and finally the diffusivity density $G(\kappa)$.

A.2. *Manipulations involving time derivatives*

The following manipulations are used to turn (5.8) into (5.9). First,

$$\nabla \times \boldsymbol{u}_2^S - \nabla \times (h_1 \boldsymbol{u}_1)/H = (v_1\xi_1)_{xx} - (u_1\eta_1)_{yy} \stackrel{t}{=} \frac{1}{2}\nabla^2(v_1\xi_1 - u_1\eta_1) \qquad \text{(A 2)}$$

follows from the definition of $\boldsymbol{u}_2^S$ and the identities $h_1/H = -\nabla\cdot\boldsymbol{\xi}_1$ and $-u_1\eta_1 = \xi_1 v_1 - (\xi_1\eta_1)_t$. Second, contracting the linear momentum equations with $\boldsymbol{\xi}_1$ yields, for $\hat{L} = 1$,

$$f(v_1\xi_1 - u_1\eta_1) \stackrel{t}{=} -\left(u_1^2 + v_1^2\right) + g\,\boldsymbol{\xi}_1\cdot\nabla h_1. \qquad \text{(A 3)}$$

This step is reminiscent of deriving the virial theorem for the linear equations. Scaling and substitution in (5.8) then yields (5.9).

REFERENCES

Balk, A. M. 2006 Wave turbulent diffusion due to the doppler shift. *J. Stat. Mech.* **P08018**.

Balk, A. M., Falkovich, G. & Stepanov, M. G. 2004 Growth of density inhomogeneities in a flow of wave turbulence. *Phys. Rev. Lett.* **92** (244504).

Batchelor, G. 1952 Diffusion in a field of homogeneous turbulence. II. The relative motion of particles. *Proc. Cambridge Philos. Soc.* **48**, 345–362.

Bühler, O. & McIntyre, M. E. 1998 On non-dissipative wave–mean interactions in the atmosphere or oceans. *J. Fluid Mech.* **354**, 301–343.

Chertkov, M., Falkovich, G., Kolokolov, I. & Lebedev, V. 1995 Statistics of a passive scalar advected by a large-scale two-dimensional velocity field: analytic solution. *Phys. Rev.* E **51** (6), 5609–5627.

Herterich, K. & Hasselmann, K. 1982 The horizontal diffusion of tracers by surface waves. *J. Phys. Oceanography* **12**, 704–712.

Kraichnan, R. H. 1970 Diffusion by a random velocity field. *Phys. Fluids* **13**, 22–32.

Ledwell, J., Watson, A. & Law, C. 1993 Evidence for slow mixing across the pycnocline from an open-ocean tracer-release experiment. *Nature* **364**, 701–703.

Ledwell, J., Watson, A. & Law, C. 1998 Mixing of a tracer in the pycnocline. *J. Geophys. Res.* **103** (C10), 21499–21529.

Majda, A. J. & Kramer, P. R. 1999 Simplified models for turbulent diffusion: theory, numerical modelling, and physical phenomena. *Phys. Rep.* **314**, 237–574.

Polzin, K. & Ferrari, R. 2004 Isopycnal dispersion in NATRE. *J. Phys. Oceanography* **34**, 247–257.

Richardson, L. F. 1926 Atmospheric diffusion shown on a distance-neighbour graph. *Proc. R. Soc. London Ser.* A **110**, 709–737.

Sanderson, B. G. & Okubo, A. 1988 Diffusion by internal waves. *J. Geophys. Res.* **93**, 3570–3582.

Sawford, B. 2001 Turbulent relative dispersion. *Ann. Rev. Fluid Mech.* **33**, 289–317.

Taylor, G. I. 1921 Diffusion by continuous movements. *Proc. London Math. Soc.* **20**, 196–212.

Toschi, F. & Bodenschatz, E. 2009 Lagrangian properties of particles in turbulence. *Ann. Rev. Fluid. Mech.* **41**, 375–404.

Vucelja, M., Falkovich, G. & Fouxon, I. 2007 Clustering of matter in waves and currents. *Phys. Rev.* E **75** (065301).

Weichman, P. & Glazman, R. 2000 Passive scalar transport by travelling wave fields. *J. Fluid Mech.* **420**, 147–200.

Whitham, G. B. 1974 *Linear and Nonlinear Waves*. John Wiley & Sons.

Yaglom, A. M. 1962 *An Introduction to the Theory of Stationary Random Functions*. Dover.

Yaglom, A. M. 1987 *Correlation Theory of Stationary and Related Random Functions. Vol 1: Basic Results*. Springer.